Stochastic Optimal Planning of Community-based Microgrid Considering Energy Justice

Cong Bai[1], *Student Member, IEEE,* Han Wang[1], Zhaoyu Wang[1], *Senior Member, IEEE*, and Yu Wang[2]
[1]*Department of Electrical and Computer Engineering,* [2]*Department of Political Science, Iowa State University, Ames, USA*
congbai@iastate.edu, hanwang6@iastate.edu, wzy@iastate.edu, yuwang@iastate.edu

***Abstract*—Low-income households (LIH), exposed to the uncertain modern grid, bear greater energy burdens and face inequitable access to reliable power compared to high-income households (HIH). This paper proposes a two-stage stochastic community-based microgrid planning (CMP) framework to boost energy justice within the system. To reduce the negative impact of income levels, a weighted energy cost model for households within the microgrid (MG) is designed. To address the multi-source uncertainty during the operation period, a two-stage stochastic framework is developed. Moreover, to assess the proposed method, the unbalanced IEEE 123 node system is employed and modified as an isolated MG. The analysis reveals the proposed model can achieve a risk-averse solution while economic optimality is guaranteed. Additionally, the designed weighted method improves the LIH's impact rate to 67.95% and decreases the total planning cost by 22.43%.**

***Index Terms*—Energy justice, Stochastic programming, Unbalanced power flow, Microgrid Planning**

I. Introduction

The concept of energy justice has gained increasing attention in the modern power grid as it aims to ensure that all communities have equitable access to affordable, reliable, and sustainable energy resources. Energy justice addresses the disproportionate burden of energy costs and limited access to clean energy faced by vulnerable groups, particularly low-income households [1]. Additionally, fuel poverty, which refers to the inability of households to afford adequate energy services, disproportionately impacts low-income and minority households, as these groups are often less energy efficient and more vulnerable to energy poverty [2]. By highlighting the importance of fairness in energy distribution, energy justice advocates for policies that consider the diverse socioeconomic conditions of different communities, fostering more inclusive and resilient energy solutions [3].

Achieving a just, clean energy transition requires proactive community engagement to ensure that benefits reach vulnerable and underresourced households. Community-based microgrid planning (CMP) has emerged as an effective approach to addressing energy justice by providing localized energy solutions that enhance resilience and ensure equitable power distribution [4]. Microgrids (MGs) are particularly well-suited to serve vulnerable communities, as they can operate independently of the larger grid, thereby improving energy access and reducing dependency on centralized power systems [5], [6]. To bridge the gap inside the communities that have long faced energy injustices, three novel equity-oriented indices are introduced to establish a CMP framework [7]. To mitigate the enormous overnight capital investment barriers in the planning process, a group of distributed energy resources (DER), including photovoltaic (PV) systems and energy storage (ES) systems, are integrated into a controllable entity to deploy renewable energy to LIH [8]. By focusing on community needs and involving local stakeholders, MG planning can incorporate energy justice principles, ensuring that marginalized groups are not left behind in transitioning to a sustainable energy future.

This work was supported in part by the National Science Foundation under 2228620.

Uncertainty is an inherent aspect of MG planning, particularly in the context of achieving energy justice. Factors such as fluctuating energy demands, variability in renewable generation, and the changing socioeconomic status of communities can significantly affect the performance and feasibility of MGs [9]. Multi-source uncertainty, including renewable energy sources (RES), such as PV, wind, tidal sources, load demand, and electricity price, is handled by Monte Carlo Simulation (MCS) to develop a stochastic energy management system for MG planning [10]. Addressing these uncertainties requires planning methodologies that integrate stochastic optimization, ensuring that MGs are designed to be adaptable and resilient in the face of diverse and unpredictable conditions [11]. Incorporating uncertainty into CMP not only enhances system reliability but also ensures that energy solutions remain equitable under different future scenarios.

Therefore, in this paper, to address the uncertainty sources during the CMP process and boost energy justice at the same time, a full two-stage stochastic CMP model is proposed. Summarily, The technical contributions of this work are as follows:

- An income-based weighted household electricity cost model is developed to boost energy justice within the community-based MG.
- A two-stage stochastic framework is proposed to handle the MG investment and operation considering the multi-source uncertainties in different scenarios.
- The three-phase unbalanced IEEE 123 node feeder is modified as an isolated MG to test and validate the proposed planning model.

The rest of this paper is organized as follows. Section II formulates the full two-stage stochastic CMP model. Section III presents the simulation setup. And then, three cases are designed and validated in Section IV. Finally, Section V concludes the whole work.

II. Mathematical Formulation

In this section, a two-stage stochastic CMP model is proposed. Firstly, the investment problem is established in the first stage. Secondly, the scenario-based operation problem considering weighted customers is formulated in the second stage. Lastly, the full two-stage stochastic model is presented.

A. First Stage Investment Problem

The available DERs include ES, PV, and diesel generator (DG), which is noted as $\mathcal{D} = \{\text{ES}, \text{DG}, \text{PV}\}$ and the candidate buses set as $\mathcal{B}^{cand}$, the investment problem in the first stage can be written as follows:

$$\min \quad F^{\text{IC}}, \tag{1}$$

$$s.t. \quad F^{\text{IC}} = F^{\text{IC},ins} + F^{\text{IC},dev}, \tag{2}$$

$$F^{\text{IC},ins} = \sum_{i \in \mathcal{B}^{cand}} \sum_{\chi \in \mathcal{D}} \left(\alpha_i^{\chi} y_i^{\chi}\right), \tag{3}$$

$$F^{\text{IC},dev} = \sum_{i \in \mathcal{B}^{cand}} \left[\sum_{\chi \in \mathcal{D}} \left(\beta^{\chi} S_{i,nom}^{\chi}\right) + \gamma^{\text{ES}} E_{i,nom}^{\text{ES}} \right], \tag{4}$$

$$y_i^{\chi} S_{\min}^{\chi} \leq S_{i,nom}^{\chi} \leq y_i^{\chi} S_{\max}^{\chi} \quad \forall i \in \mathcal{B}^{cand}, \chi \in \mathcal{D}, \tag{5}$$

$$y_i^{\text{ES}} E_{\min}^{\text{ES}} \leq E_{i,nom}^{\text{ES}} \leq y_i^{\text{ES}} E_{\max}^{\text{ES}} \quad \forall i \in \mathcal{B}^{cand}, \tag{6}$$

where $F^{\text{IC}}, F^{\text{IC},ins}, F^{\text{IC},dev}$ are the investment cost (IC), installation cost, and device cost, respectively. α_i^{χ} is the installation cost of device χ in bus i. y_i^{χ} is the binary variable to indicate whether install the device χ in bus i. β^{χ} is the rated power-based per unit price for device χ. $S_{i,nom}^{\chi}$ is the planned rated power for the device χ in bus i. γ^{ES} is the energy-based per unit price for the ES. $E_{i,nom}^{\text{ES}}$ is the planned energy capacity for the ES in bus i. $S_{\min}^{\chi}$ and $S_{\max}^{\chi}$ are the minimum and maximum rated power for single device χ. $E_{\min}^{\text{ES}}$ and $E_{\max}^{\text{ES}}$ are the minimum and maximum energy capacities for the single ES.

B. Second Stage Operation Problem

Given a finite set of stochastic scenarios $\mathcal{S}$ whose element s defines a typical daily scene representing the whole year, the scenario-based operation problem is presented as follows.

1) Modeling Net Present Value-based Operation Cost

Based on the income levels of different households, the buses containing loads within the community-based MG are partitioned into two sets, $\mathcal{B}^{\text{H}}$ and $\mathcal{B}^{\text{L}}$, which represent the high-income household (HIH) and low-income household (LIH) customers, respectively. Assume the planning period is N and the discount rate is ρ, the operation cost (OC), F_s^{OC}, in the scenario s is as follows [12], [13]:

$$F_s^{\text{OC}} = \sum_{k=1}^{N} \left[\frac{365}{(1+\rho)^k} \sum_{t \in \mathcal{T}} \epsilon_{t,s} \left(\omega^{\text{H}} \sum_{i \in \mathcal{B}^{\text{H}}} \mathbf{1}_{|\Phi_i|}^T \boldsymbol{p}_{i,t,s}^{\text{HIH}} + \omega^{\text{L}} \sum_{i \in \mathcal{B}^{\text{L}}} \mathbf{1}_{|\Phi_i|}^T \boldsymbol{p}_{i,t,s}^{\text{LIH}} \right) \right], \tag{7}$$

where $\mathcal{T}$ is the operation horizon for the typical daily scenario s. $\epsilon_{t,s}$ is the per unit electricity price at time t in the scenario s. ω^{H} and ω^{L} are the weights for the electricity cost of HIH and LIH, respectively. Φ_i is a set including the phases of bus i. $|\cdot|$ is an operator calculating the cardinality of a set. $\mathbf{1}_{|\Phi_i|}^T$ is the transpose of a column vector with all $|\Phi_i|$ elements being one. $\boldsymbol{p}_{i,t,s}^{\text{HIH}}$ and $\boldsymbol{p}_{i,t,s}^{\text{LIH}}$ are the column vectors storing the active load demands of HIH and LIH at bus i and time t in the scenario s, separately.

2) Modeling Three Phases Unbalanced Linear Power Flow

Given the buses set of the system as $\mathcal{B}$ and the child buses set of bus j as $\mathcal{B}_j$, the nodal power balance constraints for all bus $j \in \mathcal{B}$ can be written as follows:

$$\boldsymbol{p}_{j,t,s} = \sum_{k \in \mathcal{B}_j} \left(\mathbf{1}_{|\Phi_{ij}| \times |\Phi_{jk}|} \boldsymbol{p}_{jk,t,s}\right) - \boldsymbol{p}_{ij,t,s}, \tag{8a}$$

$$\boldsymbol{q}_{j,t,s} = \sum_{k \in \mathcal{B}_j} \left(\mathbf{1}_{|\Phi_{ij}| \times |\Phi_{jk}|} \boldsymbol{q}_{jk,t,s}\right) - \boldsymbol{q}_{ij,t,s}, \tag{8b}$$

$$\boldsymbol{p}_{j,t,s} = \sum_{\chi \in \mathcal{D}} \boldsymbol{p}_{j,t,s}^{\chi} - \boldsymbol{p}_{j,t,s}^{\text{HIH}} - \boldsymbol{p}_{j,t,s}^{\text{LIH}}, \tag{8c}$$

$$\boldsymbol{q}_{j,t,s} = \sum_{\chi \in \mathcal{D}} \boldsymbol{q}_{j,t,s}^{\chi} - \boldsymbol{q}_{j,t,s}^{\text{HIH}} - \boldsymbol{q}_{j,t,s}^{\text{LIH}}, \tag{8d}$$

where $\boldsymbol{p}_{j,t,s}$ and $\boldsymbol{q}_{j,t,s}$ are the column vectors storing the injection active and reactive power at bus i and time t in the scenario s, respectively. Φ_{ij} is a set including the phases of line ij. $\mathbf{1}_{|\Phi_{ij}| \times |\Phi_{jk}|}$ is a matrix with $|\Phi_{ij}|$ rows and $|\Phi_{jk}|$ columns, whose all elements are one. $\boldsymbol{p}_{ij,t,s}$ and $\boldsymbol{q}_{ij,t,s}$ are the column vectors storing the branch active and reactive power at line ij and time t in the scenario s, respectively. $\boldsymbol{p}_{j,t,s}^{\chi}$ and $\boldsymbol{q}_{j,t,s}^{\chi}$ are the active and reactive output of the device χ at bus j and time t in the scenario s, separately. $\boldsymbol{q}_{i,t,s}^{\text{HIH}}$ and $\boldsymbol{q}_{i,t,s}^{\text{LIH}}$ are the column vectors storing the reactive load demands of HIH and LIH at bus i and time t in the scenario s, respectively.

Given the line set of the system as $\mathcal{L}$, the phase voltages located at the ends of a line are combined with the following constraints:

$$\boldsymbol{v}_{j,t,s} = \boldsymbol{v}_{i,t,s}^{\Phi_{ij}} - 2\left(\boldsymbol{r}_{ij} \boldsymbol{p}_{ij,t,s} + \boldsymbol{x}_{ij} \boldsymbol{q}_{ij,t,s}\right) \quad \forall ij \in \mathcal{L}, \tag{9}$$

where $\boldsymbol{v}_{j,t,s}$ is a column vector storing the square of phase voltages at bus j and time t in the scenario s. $\boldsymbol{v}_{i,t,s}^{\Phi_{ij}}$ extracts the phase voltages from $\boldsymbol{v}_{i,t,s}$ related to Φ_{ij}. $\boldsymbol{r}_{ij}$ and $\boldsymbol{x}_{ij}$ are the matrices storing the resistance and reactance of line ij, respectively, whose computations are shown in [14].

In addition, safe operation constraints guaranteeing the steady work of the system are as follows:

$$-\boldsymbol{M}_{|\Phi_{ij}|} \leq \boldsymbol{p}_{ij,t,s} \leq \boldsymbol{M}_{|\Phi_{ij}|} \quad \forall ij \in \mathcal{L}, \tag{10a}$$

$$-\boldsymbol{M}_{|\Phi_{ij}|} \leq \boldsymbol{q}_{ij,t,s} \leq \boldsymbol{M}_{|\Phi_{ij}|} \quad \forall ij \in \mathcal{L}, \tag{10b}$$

$$\boldsymbol{v}_{j,\min} \leq \boldsymbol{v}_{j,t,s} \leq \boldsymbol{v}_{j,\max} \quad \forall j \in \mathcal{B}, \tag{10c}$$

where $\boldsymbol{M}_{|\Phi_{ij}|}$ is the column vector storing the maximum allowable value for the pass power in the line ij. $\boldsymbol{v}_{j,\min}$ and $\boldsymbol{v}_{j,\max}$ are the column vectors storing the minimum and maximum of the square of the phase voltages at the bus j, separately.

3) Modeling Energy Storage(ES) System

The planned ES system satisfies the following constraints for each bus $i \in \mathcal{B}^{cand}$:

$$\max_{n \in \Phi} \left\{ \left(p^{\mathrm{ES}}_{i,n,t,s}\right)^2 + \left(q^{\mathrm{ES}}_{i,n,t,s})^2\right) \right\} \leq \left(\tfrac{1}{3} S^{\mathrm{ES}}_{i,nom}\right)^2, \tag{11a}$$

$$SoC_{i,t,s} = SoC_{i,t-1,s} - \mathbf{1}^T_{|\Phi_i|} \boldsymbol{p}^{\mathrm{ES}}_{i,t,s} / E^{\mathrm{ES}}_{i,nom}, \tag{11b}$$

$$SoC_{\min} \leq SoC_{i,t,s} \leq SoC_{\max}, \tag{11c}$$

where $p^{\mathrm{ES}}_{i,n,t,s}$ and $q^{\mathrm{ES}}_{i,n,t,s}$ are the active and reactive output of the n-th phase of the ES system at bus i and time t in the scenario s, respectively. $SoC_{i,t,s}$ is the ES systems state of charge (SoC) at bus i and time t in the scenario s while $SoC_{\min}$ and $SoC_{\max}$ are the minimum and maximum allowable SoC, respectively.

4) Modeling Diesel Generator(DG) System

As another flexible and controllable resource at bus $i \in \mathcal{B}^{cand}$, the DG obeys the following constraints:

$$\max_{n \in \Phi_i} \left\{ \left(p^{\mathrm{DG}}_{i,n,t,s}\right)^2 + \left(q^{\mathrm{DG}}_{i,n,t,s})^2\right) \right\} \leq \left(\tfrac{1}{3} S^{\mathrm{DG}}_{i,nom}\right)^2, \tag{12}$$

where $p^{\mathrm{DG}}_{i,n,t,s}$ and $q^{\mathrm{DG}}_{i,n,t,s}$ are the active and reactive output of the n-th phase of the DG system at bus i and time t in the scenario s, individually.

5) Modeling Behind-meter Photovoltaic(PV) System

The uncertain environment affects the behind-meter PV system's active output, while its reactive output is in a fixed ratio to the former one. Given the PV systems output rate at time t in the scenario s as $\eta_{t,s}$, for bus $i \in \mathcal{B}^{cand}$, the PV system follows the constraints:

$$\boldsymbol{p}^{\mathrm{PV}}_{i,t,s} = \tfrac{1}{3} S^{\mathrm{PV}}_{i,nom} \eta_{t,s} \mathbf{1}_{|\Phi_i|} \tag{13a}$$

$$\boldsymbol{q}^{\mathrm{PV}}_{i,t,s} = 0.352 \boldsymbol{p}^{\mathrm{PV}}_{i,t,s} \tag{13b}$$

6) Modeling Per Unit Electricity Price

Given the per unit operation cost of device χ as ϵ^{χ}, the per unit electricity price at time t in the scenario s can be calculated by dividing the total generation cost by the total active output:

$$\epsilon_{t,s} = \frac{\sum_{i \in \mathcal{B}} \sum_{\chi \in \mathcal{D}} \left(\epsilon^{\chi} \mathbf{1}^T_{|\Phi_i|} \boldsymbol{p}^{\chi}_{i,t,s} \right)}{\sum_{i \in \mathcal{B}} \sum_{\chi \in \mathcal{D}} \left(\mathbf{1}^T_{|\Phi_i|} \boldsymbol{p}^{\chi}_{i,t,s} \right)}. \tag{14}$$

C. Full Formulation of Community-based Microgrid Planning (CMP)

The full two-stage stochastic CMP problem is illustrated as follows by collecting the above two parts of content:

$$\min \quad F^{\mathrm{IC}} + \sum_{s \in \mathcal{S}} \pi_s F^{\mathrm{OC}}_s, \tag{15}$$

$$s.t. \quad \text{Investment Constraints: Eq. (2)} \sim \text{(6)}, \tag{16}$$

$$\text{Operation Constraints: Eq. (7)} \sim \text{(10), (14)} \tag{17}$$

$$\text{Device Constraints: Eq. (11)} \sim \text{(13)}, \tag{18}$$

where π_s is the probability of the scenario s.

III. Microgrid (MG) Framework and Simulation Setup

In this section, the MG architecture and simulation configuration are presented. Firstly, the IEEE 123 node system-based isolated MG is illustrated. And then, the simulation parameters are detailed. Finally, the typical scenarios used for the planning problem are defined.

A. IEEE 123 Node System

The three-phase unbalanced IEEE 123 node feeder shown in Fig. 1 is modified to form the isolated community-based MG.

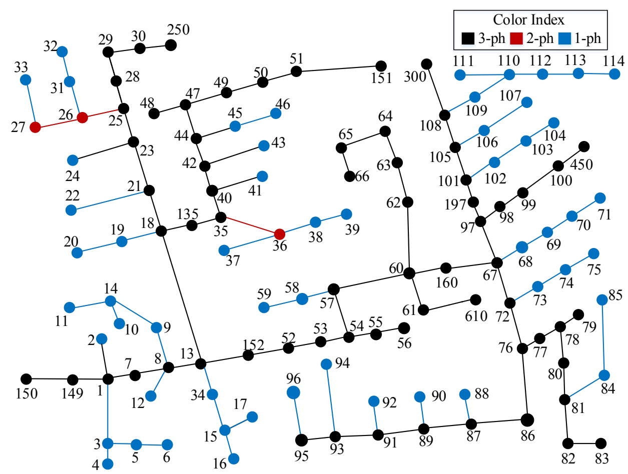

Fig. 1. Modified IEEE 123 node feeder diagram.

The minimum and maximum limits for the phase voltage are 0.95 and 1.05 per unit value, separately. The maximum allowable pass power for the branch is chosen as 600 kW. Left details about the feeder can be found in [15].

85 of the buses in the above system are connected with loads divided into two sets, shown in Table I. The base values for the weights of electricity price are $\omega^{\mathrm{H}} = 25\%$ and $\omega^{\mathrm{L}} = 75\%$. The system's maximum total active and reactive load demands are 3.49 MW and 1.99 MVar, respectively.

TABLE I
LOAD CLASSIFICATION

HIH Customers	LIH Customers
7, 10, 2, 5, 6, 12, 34, 16, 17, 19, 20, 28, 29, 33, 35, 41, 42, 43, 45, 46, 49, 50, 51, 37, 38, 39, 62, 63, 65, 52, 60, 58, 59, 107, 109, 111, 112, 113, 114, 99, 100, 75, 76, 86, 80, 82, 84, 85, 90, 92, 94, 95	1, 9, 11, 4, 24, 22, 30, 31, 32, 47, 48, 64, 66, 53, 55, 56, 102, 103, 104, 106, 98, 68, 69, 70, 71, 73, 74, 77, 79, 83, 87, 88, 96

B. Model Parameters

Assuming the planning period N is 30 years and the discount rate ρ is 6%, the device per unit price is collected in Table II.

TABLE II
DEVICE PER UNIT PRICE

Device	α(k\$)	β(k\$/MW)	γ(k\$/MWh)	ϵ(\$/kWh)
ES	100	1938.20 [16]	476.74 [16]	0.00
DG	100	2300.00 [17]	/	0.18 [17]
PV	100	1551.27 [16]	/	0.00

$S^{\chi}_{\min} = 0.1$ MVA and $S^{\chi}_{\max} = 2$ MVA for any single device while $E^{\text{ES}}_{\min} = 0.4$ MWh and $E^{\text{ES}}_{\max} = 4$ MWh for single ES. All three phases of buses in the system belong to the candidate buses set, and the simulation time step is 1 h.

C. Defined Scenarios

Four typical daily scenarios with equal probability containing the customers' behaviors and fluctuations of the PV systems are illustrated in Fig. 2.

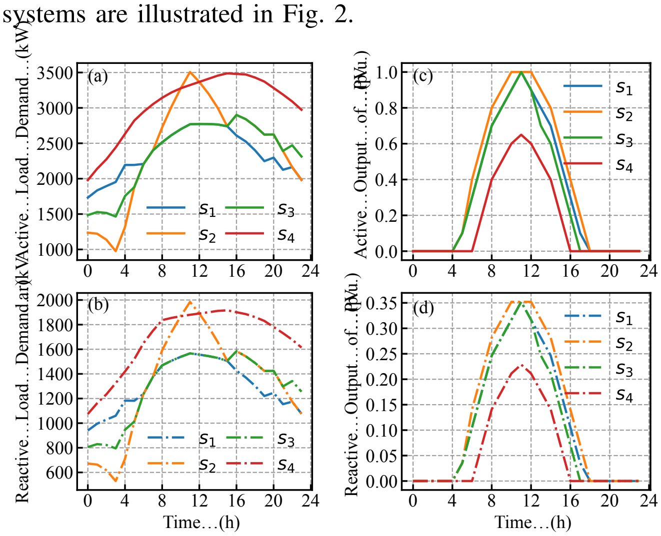

Fig. 2. Typical daily scenarios. (a) Total active load. (b) Total reactive load. (c) Active output rate of PVs. (d) Reactive output rate of PVs.

IV. NUMERICAL RESULTS

In this section, three cases are designed to validate the proposed planning method. Firstly, the risk-averse planning solution is presented. Secondly, the system performance is studied under the extreme scenario. Lastly, the sensitivity of different household weights is analyzed.

A. Case 1: Risk-averse Planning Results

By solving the two-stage stochastic CMP model, the economic optimal solution considering uncertainty is given in Table III.

All three planned ES systems have a relatively higher energy capacity than their nominal rated power, where the maximum energy capacity in bus 105 is 3.3684 MWh. In contrast, PV systems have the biggest nominal rated power among all types of devices, which are 1.5293, 1.5551, and 1.5083 MW, respectively.

Moreover, the itemized costs of each scenario are listed in Table IV to compare with the stochastic planning result.

As shown in Table IV, the stochastic planning results handle with the risks from all scenarios while the total cost is

TABLE III
RISK-AVERSE PLANNING RESULTS

No.	Type	Location	S_{nom}(MW)	E_{nom}(MWh)	Price(k\$)
1	ES	105	0.8380	3.3684	3230.06
2	ES	108	0.8181	3.3394	3177.67
3	ES	151	0.7322	2.9573	2829.01
4	DG	149	1.2777	/	2938.71
5	DG	151	1.0950	/	2518.50
6	PV	105	1.5293	/	2372.36
7	PV	108	1.5551	/	2412.38
8	PV	151	1.5083	/	2339.78

TABLE IV
ITEMIZED COST COMPARISON

Sce.	F^{IC} (k\$)		F^{OC} (k\$)	$F^{\text{IC}} + F^{\text{OC}}$ (k\$)
	$F^{\text{IC},ins}$	$F^{\text{IC},dev}$		
1	800	22075.43	1972.26	24847.69
2	700	19422.00	4063.28	24185.28
3	700	21243.99	5264.83	27208.82
4	600	19430.60	20710.33	40740.93
Stoch.	800	21818.47	8980.93	31599.40

optimized. Compared with scenario 4, the total planning cost is reduced by 22.43%.

B. Case 2: Extreme Scenario System Performance

The stochastic planning results obtained from case 1 in Section IV-A are utilized to operate the microgrid under scenario 4, which has the maximum average load demand and minimum PV output, to validate the plan's performance, shown in Fig. 3.

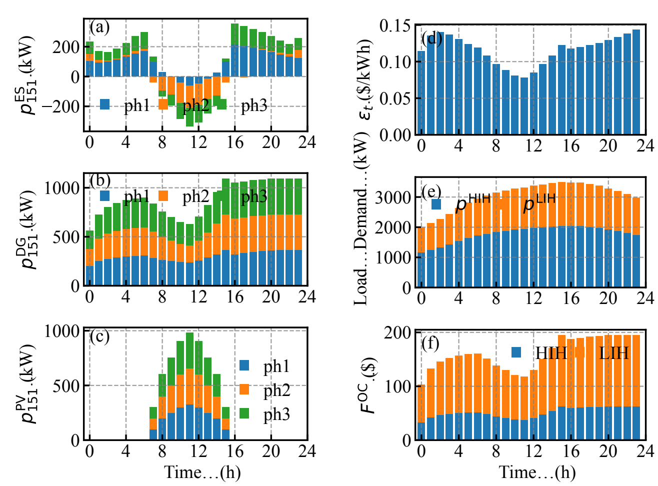

Fig. 3. System performance under extreme scenario. (a) ES active output at bus 151. (b) DG active output at bus 151. (c) PV active output at bus 151. (d) Per unit electricity price. (e) Load Demand. (f) Operation Cost.

As shown in Fig. 3 (a), one of the planned ES systems with low nominal rater power but high energy capacity by charging from 8:00 to 14:00 to move the high nominal rater power PV system's output to other operation time step. The per unit electricity price increased from 0.1180 \$/kWh at 16:00

to its peak value of 0.1436 \$/kWh at 23:00, which matches the change in ES system output.

The load demand levels of HIH and LIH customers shown in Fig. 3 (e) present that the LIH customers are inferior during the original two-stage planning problem. However, the big weight of LIH's electricity price makes LIH's operation cost matter during the planning process. The average percentage of LIH's operation cost is 67.95%.

In addition, the critical states of the MG, including phase voltages and SoC, are depicted in Fig. 4.

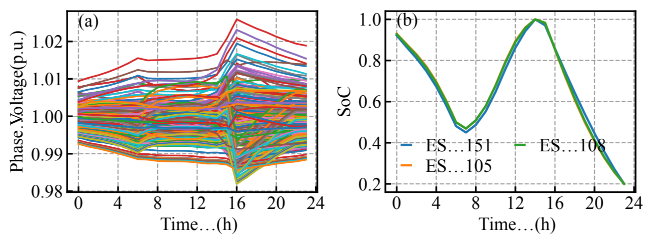

Fig. 4. System States. (a) Phase voltages. (b) State of Charge (SoC).

As illustrated in Fig. 4 (a), the phase voltages are always controlled within the safe range as Eq. (10c) required. Meanwhile, the SoC of the installed ES systems during operation is also restricted to 0.2∼1.0 as the Eq. (11c) asked.

C. Case 3: Sensitivity Analysis

Different pairs of $(\omega^{\mathrm{H}}, \omega^{\mathrm{L}})$ are adopted in the stochastic CMP to test the cost sensitivity, which is shown in Fig. 5.

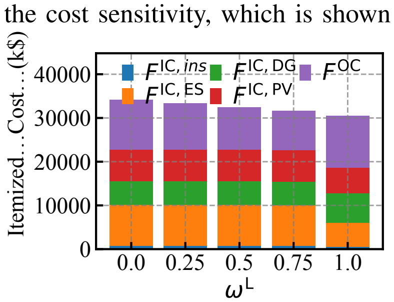

Fig. 5. Sensitivity of cost via ω^{L}.

As the value of ω^{L} increases from 0 to 0.75, the total cost of the planning problem decreases from 34133.10 k\$ to 31599.40 k\$, which is caused by the decreased operation cost, while the investment cost is almost the same. The former four plans present the same planning structure among the three types of devices, where more ES systems and PV systems help decrease LIH's energy cost. Moreover, for the pair $(\omega^{\mathrm{H}}, \omega^{\mathrm{L}})$, the higher weight on LIH means $(0.25, 0.75)$ has the best economic performance than other four pairs.

However, when the ω^{L} keeps increasing to 1.0, the planning structure is destroyed. The increased operation cost led by more investment in DG systems burdens LIH's energy cost, although LIH's low original load demand abnormally decreased the total cost.

V. Conclusion

This study investigates energy justice's impact on the CMP problem with multi-source uncertainty. Firstly, a weighted energy cost model is designed to consider the impact of income levels. And then, a full two-stage stochastic CMP model is established. Finally, the proposed method is assessed on the modified IEEE 123 node system-based MG. The case study analysis presents that the risk-averse plan improves the LIH's impact rate to 67.95% and reduces 22.43% of the total cost.

References

[1] M. Apergi, L. Eicke, A. Goldthau, M. Hashem, S. Huneeus, R. Lima de Oliveira, M. Otieno, E. Schuch, and K. Veit, "An energy justice index for the energy transition in the global south," *Renewable and Sustainable Energy Reviews*, vol. 192, p. 114238, 2024.

[2] T. G. Reames, "Targeting energy justice: Exploring spatial, racial/ethnic and socioeconomic disparities in urban residential heating energy efficiency," *Energy Policy*, vol. 97, pp. 549–558, 2016.

[3] B. K. Sovacool, S. Carley, and L. Kiesling, "Energy justice beyond the wire: Exploring the multidimensional inequities of the electrical power grid in the united states," *Energy Research Social Science*, vol. 111, p. 103474, 2024.

[4] B. Brickhouse, G. Siegfried, E. Torres-Soto, and B. Williams, "Community participation in the clean energy transition: A procedural justice perspective on meaningful involvement," *IEEE Power and Energy Magazine*, vol. 22, no. 4, pp. 75–84, 2024.

[5] Z. Wang, B. Chen, J. Wang, M. M. Begovic, and C. Chen, "Coordinated Energy Management of Networked Microgrids in Distribution Systems," *IEEE Transactions on Smart Grid*, vol. 6, no. 1, pp. 45–53, 2015.

[6] Z. Wang and J. Wang, "Self-Healing Resilient Distribution Systems Based on Sectionalization Into Microgrids," *IEEE Transactions on Power Systems*, vol. 30, no. 6, pp. 3139–3149, 2015.

[7] J. S. G. L. K. W. Behnam Sabzi, Farzane Ezzati and Z. S. Dong, "Energy equity-centered planning of community microgrids," *TechRxiv*, vol. 35, no. 1, pp. 13–29, 2024.

[8] A. M. Abdelbary, L. Manglicmot, O. Kanwhen, and A. A. Mohamed, "Community-centric distributed energy resources for energy justice and decarbonization in dense urban regions," *Energy Reports*, vol. 11, pp. 1742–1751, 2024.

[9] M. Hamidieh and M. Ghassemi, "Microgrids and resilience: A review," *IEEE Access*, vol. 10, pp. 106 059–106 080, 2022.

[10] P. Hajiamoosha, A. Rastgou, S. Bahramara, and S. M. Bagher Sadati, "Stochastic energy management in a renewable energy-based microgrid considering demand response program," *International Journal of Electrical Power Energy Systems*, vol. 129, p. 106791, 2021.

[11] E. G. Vera, C. A. Cañizares, M. Pirnia, T. P. Guedes, and J. D. M. Trujillo, "Two-stage stochastic optimization model for multi-microgrid planning," *IEEE Transactions on Smart Grid*, vol. 14, no. 3, pp. 1723–1735, 2023.

[12] L. Romero Rodríguez, J. Sánchez Ramos, M. Guerrero Delgado, J. L. Molina Félix and S. Álvarez Domínguez, "Mitigating energy poverty: Potential contributions of combining PV and building thermal mass storage in low-income households," *Energy Conversion and Management*, vol. 173, pp. 65–80, 2018.

[13] J. C. Romero, P. Linares, A. F. Rodriguez-Matas, and M. Perez-Bravo, "Illustrating the conflicts between energy poverty and decarbonization in the energy transition. A case example in Spain," *Energy*, vol. 314, p. 134204, 2025.

[14] R. Cheng, Z. Wang, Y. Guo, and Q. Zhang, "Online voltage control for unbalanced distribution networks using projected newton method," *IEEE Transactions on Power Systems*, vol. 37, no. 6, pp. 4747–4760, 2022.

[15] K. P. Schneider, B. A. Mather, B. C. Pal, C.-W. Ten, G. J. Shirek, H. Zhu, J. C. Fuller, J. L. R. Pereira, L. F. Ochoa, L. R. de Araujo, R. C. Dugan, S. Matthias, S. Paudyal, T. E. McDermott, and W. Kersting, "Analytic Considerations and Design Basis for the IEEE Distribution Test Feeders," *IEEE Transactions on Power Systems*, vol. 33, no. 3, pp. 3181–3188, 2018.

[16] N. R. E. L. (NREL). (2024) Renewable electricity futures study. [Online]. Available: https://www.nrel.gov/analysis/re-futures.html

[17] U. E. I. Administration. (2023, March) Cost and performance characteristics of new generating technologies, annual energy outlook 2023. [Online]. Available: https://www.eia.gov/outlooks/aeo/assumptions/pdf/elec_cost_perf.pdf